Greater cellular stiffness in fibroblasts from patients with idiopathic pulmonary fibrosis

Jaffar, Jade; Yang, Sung-Hee; Kim, Sally Yunsun; Kim, Hae-Won; Faiz, Alen; Chrzanowski, Wojciech; Burgess, Janette K

Published in:
American Journal of Physiology - Lung Cellular and Molecular Physiology

DOI:
10.1152/ajplung.00030.2018

Am J Physiol Lung Cell Mol Physiol 315: L59–L65, 2018.
First published March 8, 2018; doi:10.1152/ajplung.00030.2018.

RAPID REPORT

Greater cellular stiffness in fibroblasts from patients with idiopathic pulmonary fibrosis

Jade Jaffar,[1,2,3] Soung-Hee Yang,[4,5] Sally Yunsun Kim,[6] Hae-Won Kim,[4,5] Alen Faiz,[1,7,8] Wojciech Chrzanowski,[4,6]* and Janette K. Burgess[1,7,9]*

[1]*Woolcock Institute of Medical Research, The University of Sydney, Sydney, Austrailia;* [2]*Department of Allergy, Immunology and Respiratory Medicine, The Alfred Hospital, Melbourne, Australia;* [3]*Department of Immunology and Pathology, Monash University, Melbourne, Australia;* [4]*Department of Nanobiomedical Science and Global Research Center for Regenerative Medicine, Dankook University, Cheonan, Republic of Korea;* [5]*Institute of Tissue Regeneration Engineering and College of Dentistry, Dankook University, Cheonan, Republic of Korea;* [6]*Faculty of Pharmacy, The University of Sydney Nano Institute, The University of Sydney, Sydney, Australia;* [7]*The University of Groningen, University Medical Center Groningen, Department of Pathology and Medical Biology, Groningen Research Institute for Asthma and COPD, Groningen, The Netherlands;* [8]*The University of Groningen, University Medical Center Groningen, Department of Pulmonology, Groningen Research Institute for Asthma and COPD, Groningen, The Netherlands; and* [9]*Discipline of Pharmacology, The University of Sydney, Sydney, Australia*

Submitted 22 January 2018; accepted in final form 22 February 2018

Jaffar J, Yang SH, Kim SY, Kim HW, Faiz A, Chrzanowski W, Burgess JK. Greater cellular stiffness in fibroblasts from patients with idiopathic pulmonary fibrosis. *Am J Physiol Lung Cell Mol Physiol* 315: L59–L65, 2018. First published March 8, 2018; doi:10.1152/ajplung.00030.2018.—Idiopathic pulmonary fibrosis (IPF) is a lethal lung disease involving degenerative breathing capacity. Fibrotic disease is driven by dysregulation in mechanical forces at the organ, tissue, and cellular level. While it is known that, in certain pathologies, diseased cells are stiffer than healthy cells, it is not known if fibroblasts derived from patients with IPF are stiffer than their normal counterparts. Using IPF patient-derived cell cultures, we measured the stiffness of individual lung fibroblasts via high-resolution force maps using atomic force microscopy. Fibroblasts from patients with IPF were stiffer and had an augmented cytoskeletal response to transforming growth factor-β1 compared with fibroblasts from donors without IPF. The results from this novel study indicate that the increased stiffness of lung fibroblasts of IPF patients may contribute to the increased rigidity of fibrotic lung tissue.

atomic force microscopy; cytoskeleton; fibroblasts; idiopathic pulmonary fibrosis; α-smooth muscle actin

INTRODUCTION

Pulmonary fibrosis, a permanent consequence of a range of lung diseases, affects the lung interstitium: the specialized network of tissue that surrounds the air sacs (alveoli) and their corresponding blood vessels. In idiopathic pulmonary fibrosis (IPF), the excessive production of extracellular matrix (ECM) by lung myofibroblasts leads to the progressive stiffening of the tissue (21), resulting in the loss of lung function. However, few studies have investigated the stiffness of the fibroblast's cytoskeleton, which influences the overall stiffness of the tissue (1, 10, 19).

A myofibroblast's ability to contract is a function of its cytoskeleton and these forces are largely generated by α-smooth muscle actin (α-SMA) in stress fibers (12). Compared with fibroblasts derived from patients without fibrosis [nondiseased control (NDC) fibroblasts], fibroblasts from patients with IPF (IPF fibroblasts) have increased basal expression of α-SMA (27). Therefore, we hypothesized that IPF fibroblasts would also have greater internal cytoskeletal stiffness than NDC fibroblasts.

Transforming growth factor-β1 (TGF-β1) increases α-SMA expression in mesenchymal cells (7) and cell stiffness of epithelial cells (31). Lung fibroblasts obtain information about their surrounding physical environment through their cytoskeleton (3); thus a fibrotic ECM potentially activates a continuous loop where the increased stiffness of the fibroblasts' immediate microenvironment causes alterations in cell behavior (20, 24).

The aim of this study was to measure the nanomechanical properties of primary lung fibroblasts using high-resolution, atomic force microscopy. To investigate cell cytoskeletal dysregulation in fibrotic disease, primary lung fibroblasts from patients with IPF were compared with fibroblasts from age- and sex-matched individuals with no history of fibrotic lung disease. The cytoskeletal rearrangements of α-SMA were examined before and after stimulation with TGF-β1.

METHODS

Primary Lung Fibroblast Culture

Lung tissue was obtained from patients with IPF or from patients undergoing resection and donors whose lungs were deemed unsuitable for transplantation and who, or whose next of kin, provided written, informed consent. The University of Sydney Human Research Ethics Committee (No. 2012/946) and the Alfred Hospital Ethics Committee (No. 468/14) provided ethical approval. Donor demographical information is in Table 1.

Fibroblasts were isolated from distal lung parenchyma as previously described (9).

* W. Chrzanowski and J. K. Burgess contributed equally to this work.
Address for reprint requests and other correspondence: J. Burgess Dept. of Pathology and Medical Biology, Groningen Research Institute for Asthma and COPD, Univ. Medical Center, Univ. of Groningen, Groningen, 9713GZ Groningen, The Netherlands (e-mail: j.k.burgess@umcg.nl).

Table 1. *Demographics of patients from whom fibroblasts were derived*

Patient No.	Sex	Age**	Diagnosis	History of Smoking?	FEV_1	FVC	DL_{CO}	CPI
NDC1	N/A	39	Healthy	Yes	N/A	N/A	N/A	N/A
NDC2	Male	69	Healthy	Yes	N/A	N/A	N/A	N/A
NDC3	Female	60	Healthy	Yes	N/A	N/A	N/A	N/A
NDC4	Female	28	Healthy	Yes	N/A	N/A	N/A	N/A
NDC5	N/A	N/A	Healthy	N/A	N/A	N/A	N/A	N/A
*NDC6**	Male	66	NSCLC	N/A	N/A	N/A	N/A	N/A
*NDC7**	Male	60	NSCLC	Yes	77	97	N/A	N/A
*NDC8**	Male	61	NSCLC	Yes	75	77	N/A	N/A
IPF1	Male	65	IPF	Yes	48	43	36	61.1
IPF2	Male	61	IPF	Yes	57	48	47	54.4
IPF3	Male	69	IPF	Yes	86	86	17	63.6
IPF4	Male	63	IPF	Yes	N/A	N/A	19	N/A
IPF5	Female	56	IPF	No	53	47	16	73.7
*IPF6**	Male	55	IPF	Yes	52	48	26	66.3
*IPF7**	Male	58	IPF	Yes	57	51	18	71.7
*IPF8**	Male	58	IPF	Yes	55	46	18	73.6

Lung function measurements are presented in percent predicted values. FEV_1, forced expiratory volume in 1 s; FVC, forced vital capacity; DL_{CO}, diffusing capacity of carbon monoxide; CPI, composite physiologic index; IPF, idiopathic pulmonary fibrosis; NSCLC, nonsmall cell lung cancer; NDC, nondiseased control; N/A, not available. *Participants from whom fibroblasts used in the atomic force microscopy experiments were derived. **Unpaired, two-tailed *t*-test ($n = 8$/group; $P = 0.3$).

All cultures tested negative for mycoplasma before use in experiments, and only cell cultures at less than six passages were used.

Cell Experimentation

Primary fibroblasts were seeded in 5% FBS/1% antibiotics/DMEM for 72 h and then quiesced in 0.1% FBS/1% penicillin-streptomycin/DMEM (quiescing media) for 24 h. Fresh quiescing media, with or without 10 ng/ml activated TGF-β1 (R&D Systems), was added for 72 h. Some fibroblasts were seeded on tissue culture plastic (TCP) coated with 0.002 g/ml gelatin powder (Ajax Chemicals) in sterile water for 1 h at room temperature before being rinsed twice with sterile PBS (Invitrogen) immediately before seeding.

After treatment, cells were rinsed twice with sterile PBS and fixed in freshly made 4% (vol/vol) paraformaldyhyde (Sigma, Melbourne, Australia) in PBS for 15 min at room temperature. Cells were rinsed twice with PBS and stored in sterile PBS at 4°C until further experimentation. All samples for nanomechanical experiments were prepared at the same time.

Cell Morphology and Stiffness Measurements

Cell morphology. Detailed three-dimensional morphology of the cells was acquired using molecular force probe microscopy (MFP-3D-Bio, Asylum Research, Santa Barbara, CC). Cells were located using light microscopy and imaged using atomic force microscopy operating in contact mode using AppNano (HYDRA-ALL) probes with nominal spring constant 0.012 N/m. Sensitivity and spring constant calibrations of the probe were performed immediately before cells were indented.

Nanomechanical analysis of cell stiffness. To probe the nanomechanical properties of cells, MFP-3D-Bio equipped with HYDRA-ALL probe was used with the probe deflection set to 200 nm. To eliminate dragging effects of and minimize interaction of fluid on the measurements, the approach speed was set at 200 nm/s.

For each sample a minimum of 5 areas (50×50 μm) were scanned each including several cells, for each area 6,400 (80×80) force curves were recorded, enabling the creation of force-volume "maps" for each sample.

The elastic properties (Young's modulus) of the cells were determined by fitting each of the 6,400 force curves to a contact-mechanics model (16). To take into account probe tip-sample adhesion forces (15), the Derjaguin-Muller-Toporov model was used (6), with the Poisson ratio of all the samples set to 0.5, the archetypical value for biological samples (2, 11).

Quantification of stiffness measurements. Force maps underwent log-transformed regression analysis using the corresponding histogram plot of stiffness measurements (17). Only force maps that obtained a significant goodness of fit (R^2) value ≥ 0.95 ($P < 0.05$) were included.

Immunocytochemistry

Fibroblasts were labeled with anti-α-SMA (Abcam), detected with a secondary antibody conjugated to AlexaFluor-594 (Abcam) and anti-vimentin conjugated to AlexaFluor-488 (BD Biosciences). Nuclei were labeled with Hoescht 32555 (Invitrogen). Each cell line was imaged two to three times in different areas, using the same microscope settings on the same day. Cells were imaged using a Nikon A1r si confocal microscope (Olympus) in galvanometric scanning mode with a ×40 water immersion objective with coverslip correction collar (Nikon CFI Apo Lambda S 40X LWD WI, 1.15 NA). Z-stack images were combined using ImageJ software (version 1.50a; National Institutes of Health).

Fibroblasts in 96-well plates were permeabilized with 0.1% (vol/vol) Triton X-100 (Sigma) before incubation with mouse anti-α-SMA and rabbit anti-GAPDH concurrently. The next day, anti-mouse IgG-790 fluorochrome and anti-rabbit-680 fluorochrome were added. Plates were imaged using an Odyssey Infrared scanner (Li-Cor) and quantification performed by Image Studio (version 4; Li-Cor), with the intensity of the 800 channel set at 5 and the 700 channel set to 3. Images were scanned at an offset of 3 mm with a resolution of 169 μm.

Quality Control and Statistical Analysis

Statistical analysis was performed using SPSS (version 22; IBM), GraphPad Prism 6 (GraphPad, La Jolla, CA), and Microsoft Excel (Microsoft, Redmond, CA).

To account for the intrinsic variability of primary human lung fibroblasts, we performed intraclass correlation coefficient analysis on $n = 10$ cells. With the use of a two-way mixed effects model with experimental error considered consistent and patient variability considered random, the intraclass correlation coefficient was 0.71 (degrees of freedom = 9, $P = 0.046$), indicating a good degree of reliability within this data set (32).

To avoid bias in data collection, probing of samples was undertaken in random order by a researcher blinded to disease and treatment. In addition, two-way repeated-measures ANOVA was used to ensure there were no differences in the quality of data between groups. In total, 37 force maps, totaling 236,800 force measurements, of 50-μm^2 areas across cells from $n = 3$ IPF and $n = 3$ NDC with similar gross morphology were collected for analysis.

The results in this study were obtained from a total of 102,459 individual force curves, of which 72,757 were used to generate linear regression equations with an average R^2 value of 0.98.

Differences in cell stiffness between NDC and IPF fibroblasts were assessed using unpaired *t*-tests on the stiffness frequencies calculated from measurements that accounted for the 15th to 85th cumulative frequency percentiles. Stiffness frequency was defined as the stiffness (Pascals) multiplied by the number of points measured (counts).

The effects of TGF-β1 on cell stiffness and α-SMA expression were assessed using ratio paired *t*-tests with the unstimulated condition as control. $P < 0.05$ was considered significant.

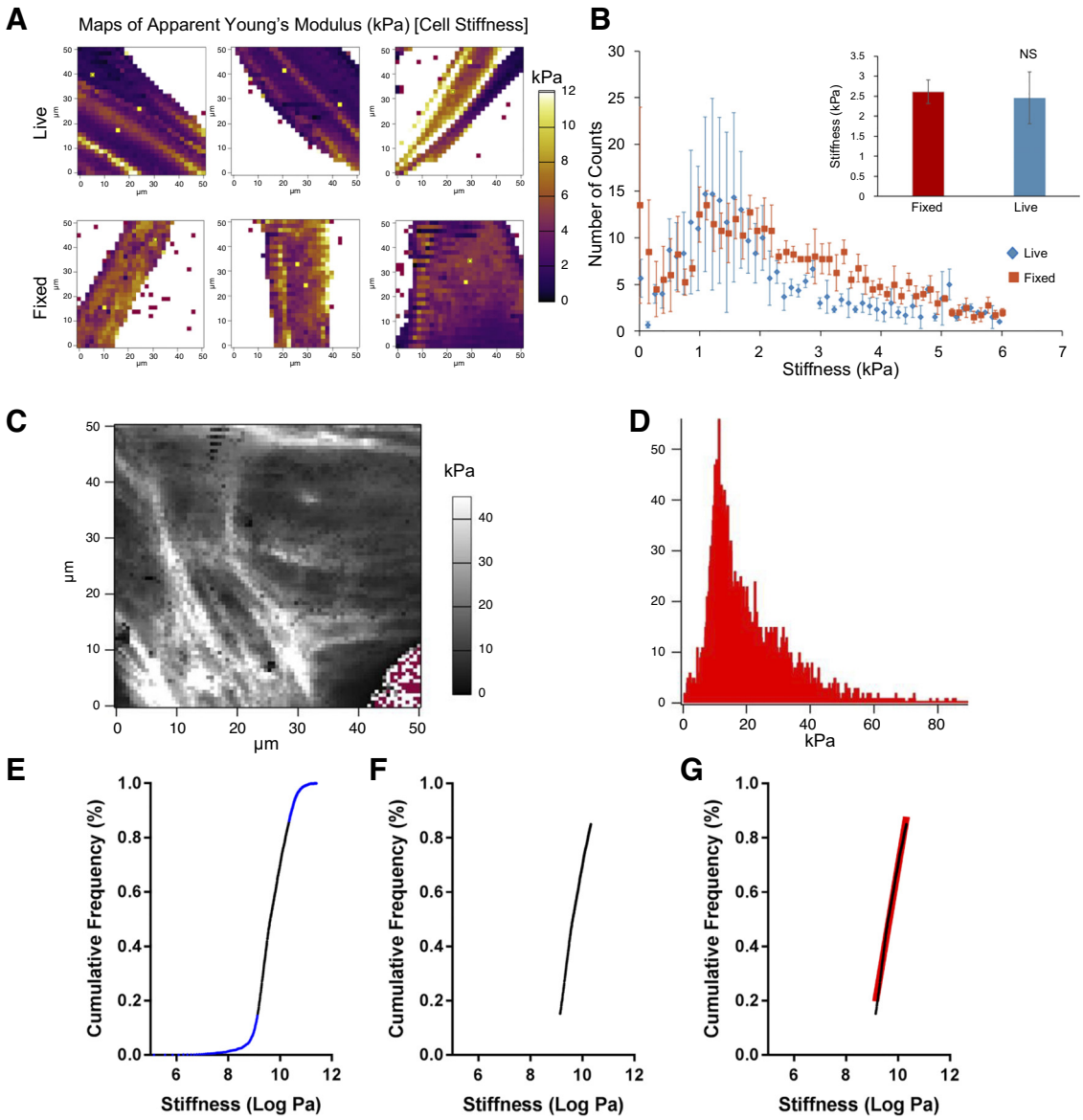

H

	Non-diseased Control (NDC)		Idiopathic Pulmonary Fibrosis (IPF)		
Patient Diagnosis (n=3 each group)	Unstimulated	TGFβ1	Unstimulated	TGFβ1	P Value
Mean (SD) number of force curves generated	3920 (1464)	8661 (5328)	5577 (1272)	4683 (1145)	ns
Mean (SD) number of force curves included in linear regression	2757 (1041)	6136 (3737)	3940 (869)	3385 (733)	ns
Mean (SD) value of linear regression constant (R^2)	0.987 (0.02)	0.981 (0.03)	0.981 (0.03)	0.990 (0.02)	ns

Fig. 1. Quantification of cell cytoskeletal stiffness. Cell stiffness was measured on fixed and live cells. *A*: representative plots. *B*: average data. *C*: representative data of an idiopathic pulmonary fibrosis (IPF) fibroblast captured using atomic force microscopy. Points marked in red show where stiffness was not measured. *D*: for each 50-μm^2 area probed, 6,400 surface points were measured, generating a force map. Measurements from each force map were quantified on histograms. *E*: histogram analysis of *D* is shown graphically; stiffness values are log normal transformed and plotted against cumulative frequency. *F*: stiffness values between the 15th and 85th percentiles were used in the linear regression model. *G*: the calculated linear regression line was overlaid in red. *H*: quality control analysis on the total data set used in this study. NDC, nondiseased control; TGF-β1, transforming growth factor-β1. *P* values are for repeated-measures two-way ANOVA investigating disease and treatment.

RESULTS

In this study, we demonstrate through molecular force probing that the stiffness of fibroblasts from patients with IPF is greater than that of fibroblasts from NDC donors.

Due to the prolonged scanning time required (~4 h) for high-resolution mechanical mapping of cells (23), fixation was necessary. Our preliminary data showed that there was no change in apparent Young's modulus (cellular stiffness) and less variability after fixation (Fig. 1, *A* and *B*).

For data analysis, the histograms of each force map (Fig. 1, *C* and *D*) were subjected to linear regression analysis (Fig. 1, *E–G*). Importantly, quality control measurements (Fig. 1*H*) indicated that there were no differences in the number of force maps or points of stiffness measured between the two disease groups and treatments.

This study sampled lung tissue from patients with IPF on the severe end of the disease spectrum, reflected in the clinical parameters in Table 1; IPF patients had a diffusion limit of carbon monoxide of 21% predicted, consistent with patients with a diffusion limit of carbon monoxide <35% predicted being considered to have severe, end-stage disease (25).

Furthermore, because IPF is a disease often associated with smoking (18), it is important that the NDC donors used in the study had a history of smoking. IPF is a disease of primarily older individuals (18), and normal aging-related changes are known to impact on cell stiffness (29). In our study, there was no difference in age between the IPF and NDC donors (Table 1).

Mechanoperception (cellular sensing of its microenvironment) can dictate cell behavior. We compared cell stiffness on 0.2% gelatin (soft) vs. TCP. There was no difference in internal cell stiffness between IPF and NDC fibroblasts on 0.2% gelatin. Strikingly, compared with gelatin, NDC fibroblasts were 115% softer on TCP, while IPF fibroblasts did not respond to the change in surface stiffness (Table 2). Our data show that the average internal cell cytoskeletons from patients with IPF were stiffer than those from NDC on TCP (Fig. 2*A*).

The differences in cytoskeletal stiffness were more pronounced after fibroblasts were treated with TGF-β1, a profibrotic cytokine that induces cytoskeletal rearrangement in fibroblasts (7, 12). Although both groups became stiffer after stimulation, IPF fibroblasts were nearly 15 times stiffer than NDC fibroblasts following TGF-β1 exposure (Fig. 2*A* and Table 2).

When the topography measurements were combined with the stiffness values, high-resolution, three-dimensional force maps were generated simulating the surface features of the 50 μm^2 scanned with overlaid color-scale stiffness information (Fig. 2*B*). Both IPF and NDC fibroblasts changed morphology following TGF-β1 stimulation. Although similar in gross morphology, IPF fibroblasts were significantly stiffer and increases in surface stiffness were seen over the entire 50 μm^2 measured.

Treatment with TGF-β1 induced α-SMA expression in both populations although bundles of α-SMA-positive fibers appeared more prominent in IPF compared with NDC fibroblasts (Fig. 2*C*). At the population level, IPF fibroblasts expressed higher levels of α-SMA than NDC fibroblasts (Fig. 2*D*), while TGF-β1 induced upregulated α-SMA in both NDC and IPF fibroblasts.

DISCUSSION

Global mortality from IPF is progressively increasing. The mechanisms governing fibroblast behavior in fibrotic lung disease are not fully understood, consequently current treatments have limited efficacy to prevent, or reverse, the fibrotic process (14, 25, 26). Our study points to an exaggerated physical response of IPF fibroblasts to TGF-β1 as a novel factor driving pathology, potentially resulting in increased tissue stiffening.

Altered fibroblast behavior is recognized in the context of IPF (1, 10), making differences in cytoskeletal regulation and mechanoperception rational therapeutic targets (33). The actin cytoskeleton confers important cellular properties, including contractility and motility (13).

In this study, we show that primary IPF fibroblasts are stiffer than NDC fibroblasts implying that in IPF the increase in individual fibroblast stiffness may contribute to an increase in overall fibrotic tissue stiffness, not a novel concept in fibrosis pathology (22, 33). In support of this, when normal lungs are decellularized, they maintain 81% of their native stiffness (indicating the cellular contribution is 19% of the native lung stiffness). When IPF lungs are decellularized, they only maintain 44% stiffness (4). Our study presents the possibility that the IPF fibroblasts themselves are stiffer.

The increase in stiffness we measured on the nanoscale in the IPF fibroblasts has implications on a tissue level. It is possible that a sustained increased stiffness of a single cell propagates alterations via mechanoperception to other fibroblasts in the immediate microenvironment. Given increased ECM production is one response to a stiffer environment (5), this may generate a profibrotic feedback loop in IPF lung tissue (24). It is not currently know if the increased stiffness of the IPF fibroblast is a response to an aberrant wound healing response (ECM deposition) or if the cell is inherently different in an IPF patient. The lung is a highly mechanical organ in which the architecture determines its functionality (8). Increased fibroblast stiffness may disrupt the tissue architecture

Table 2. *Adjusted mean stiffness values of fibroblasts from IPF and NDC under different conditions*

	NDC		IPF		
Surface/Treatment	Adjusted mean, kPa	(95% CI)	Adjusted mean, kPa	(95% CI)	Adjusted *P* Value for Pairwise Comparison
Gelatin	1.87	(1.64–2.13)	2.16	(1.90–2.46)	0.6858
TCP	0.87	(0.74–1.02)	1.74	(1.52–2.00)	<0.0001
TCP + TGF-β1	2.84	(2.44–3.31)	30.95	(27.72–34.54)	<0.0001

Adjusted mean stiffness values were calculated as the mean value between log normalized stiffness measurements for the 15th to 85th percentiles of each fibroblast line. IPF, idiopathic pulmonary fibrosis; TGF-β1, transforming growth factor-β1, NDC nondiseased control; TCP, tissue culture plastic; CI, confidence interval. Two-way ANOVA was performed, and the adjusted *P* value for the effect of cell disease type within treatment was calculated. $P \leq 0.05$ was considered significant.

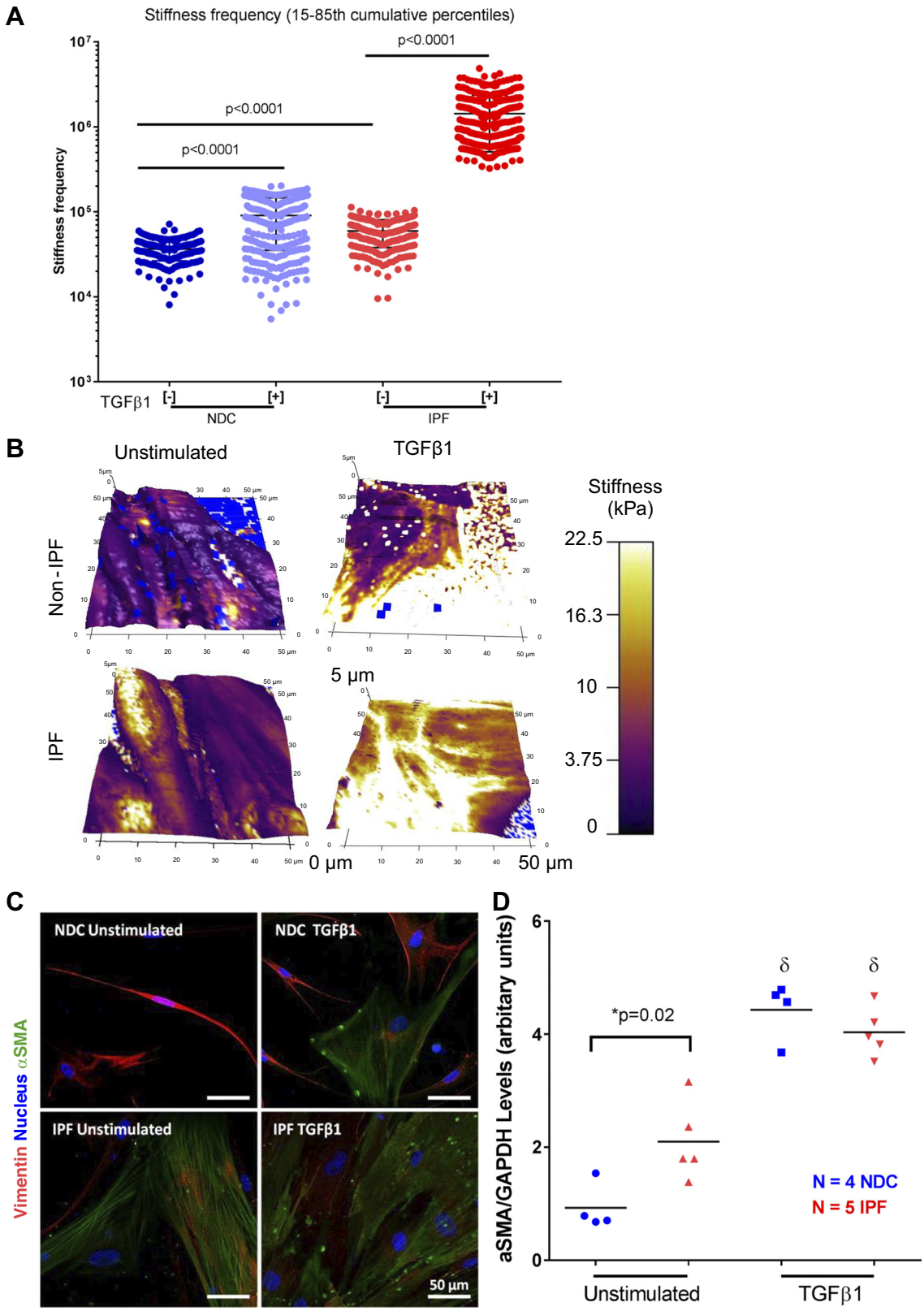

Fig. 2. Idiopathic pulmonary fibrosis (IPF) fibroblasts are stiffer than nondiseased control (NDC) fibroblasts. *A*: cell cytoskeletal stiffness frequency of $n = 3$ IPF and $n = 3$ NDC fibroblasts measured before and after transforming growth factor-β1 (TGF-β1) treatment. *B*: Representative high-resolution force maps of stiffness of IPF and NDC fibroblasts measured by atomic force microscopy. *C* and *D*: representative images (*C*) and in cell Western analysis (*D*) of α-smooth muscle actin (α-SMA) in $n = 5$ IPF and $n = 4$ NDC fibroblasts measured before and after TGF-β1 treatment. *P* values are for repeated-measures two-way ANOVA investigating disease (*) and treatment (δ).

and cause corruption of mechanically-derived signals which normally transmit through the ECM (8).

The IPF fibroblasts did not exhibit mechanoresponsiveness between a soft and hard surface, a change that was observed with NDC fibroblasts. The IPF fibroblasts showed augmented cytoskeletal responses to TGF-β1, increasing cell stiffness to a greater extent than NDC fibroblasts, indicating that the lack of mechanoresponsiveness in the IPF fibroblasts was not due to defective cytoskeletal machinery. IPF is more prevalent in older individuals (28) and normal aging-related changes share similar mechanisms with lung fibrosis (30). Skin fibroblasts from aged individuals are 60% stiffer than fibroblasts from younger patients (29). However, as there were no age differences between the NDC or IPF fibroblast donors, we can infer that the alterations in cell cytoskeletal response observed were disease related.

This is the first study to show that cell cytoskeletal regulation in IPF fibroblasts is different to that in NDC fibroblasts, possibly contributing to the increased lung stiffness in IPF. New knowledge about the differences in responses of IPF cells to profibrotic stimuli is critical for understanding underlying mechanisms to prevent or reverse disease development.

ACKNOWLEDGMENTS

We acknowledge Brock Patton's assistance with research and manuscript preparation and the Monash Micro Imaging platform for technical assistance with confocal microscopy.

GRANTS

This study was supported by National Health and Medical Research Council, Australia Fellowship No. 1032695 (to J. K. Burgess), the University of Groningen and European Union cofunded Rosalind Franklin Fellowship (to J. K. Burgess), RESPIRE2 fellowship cofunded by the European Respiratory Society and the European Union (to A. Faiz), and Longfonds Junior Investigators Grant 4.2.16.132JO (to A. Faiz).

DISCLOSURES

No conflicts of interest, financial or otherwise, are declared by the authors.

AUTHOR CONTRIBUTIONS

J.J., W.C., and J.K.B. conceived and designed research; J.J., S.-H.Y., S.Y.K., and W.C. performed experiments; J.J., S.-H.Y., S.Y.K., A.F., W.C., and J.K.B. analyzed data; J.J., S.-H.Y., S.Y.K., H.-W.K., A.F., W.C., and J.K.B. interpreted results of experiments; J.J., S.Y.K., W.C., and J.K.B. prepared figures; J.J., A.F., W.C., and J.K.B. drafted manuscript; J.J., S.-H.Y., S.Y.K., H.-W.K., A.F., W.C., and J.K.B. edited and revised manuscript; J.J., S.-H.Y., S.Y.K., H.-W.K., A.F., W.C., and J.K.B. approved final version of manuscript.

REFERENCES

1. **Álvarez D, Cárdenes N, Sellarés J, Bueno M, Corey C, Hanumanthu VS, Peng Y, D'Cunha H, Sembrat J, Nouraie M, Shanker S, Caufield C, Shiva S, Armanios M, Mora AL, Rojas M.** IPF lung fibroblasts have a senescent phenotype. *Am J Physiol Lung Cell Mol Physiol* 313: L1164–L1173, 2017. doi:10.1152/ajplung.00220.2017.
2. **Babahosseini H, Ketene AN, Schmelz EM, Roberts PC, Agah M.** Biomechanical profile of cancer stem-like/tumor-initiating cells derived from a progressive ovarian cancer model. *Nanomedicine (Lond)* 10: 1013–1019, 2014. doi:10.1016/j.nano.2013.12.009.
3. **Balestrini JL, Chaudhry S, Sarrazy V, Koehler A, Hinz B.** The mechanical memory of lung myofibroblasts. *Integr Biol* 4: 410–421, 2012. doi:10.1039/c2ib00149g.
4. **Booth AJ, Hadley R, Cornett AM, Dreffs AA, Matthes SA, Tsui JL, Weiss K, Horowitz JC, Fiore VF, Barker TH, Moore BB, Martinez FJ, Niklason LE, White ES.** Acellular normal and fibrotic human lung matrices as a culture system for in vitro investigation. *Am J Respir Crit Care Med* 186: 866–876, 2012. doi:10.1164/rccm.201204-0754OC.
5. **Chiquet M, Renedo AS, Huber F, Flück M.** How do fibroblasts translate mechanical signals into changes in extracellular matrix production? *Matrix Biol* 22: 73–80, 2003. doi:10.1016/S0945-053X(03)00004-0.
6. **Derjaguin BV, Muller VM, Toporov YP.** Effect of contact deformations on the adhesion of particles. *J Colloid Interface Sci* 53: 314–316, 1975. doi:10.1016/0021-9797(75)90018-1.
7. **Desmoulière A, Geinoz A, Gabbiani F, Gabbiani G.** Transforming growth factor-beta 1 induces alpha-smooth muscle actin expression in granulation tissue myofibroblasts and in quiescent and growing cultured fibroblasts. *J Cell Biol* 122: 103–111, 1993. doi:10.1083/jcb.122.1.103.
8. **Faffe DS, Zin WA.** Lung parenchymal mechanics in health and disease. *Physiol Rev* 89: 759–775, 2009. doi:10.1152/physrev.00019.2007.
9. **Ge Q, Chen L, Jaffar J, Argraves WS, Twal WO, Hansbro P, Black JL, Burgess JK, Oliver B.** Fibulin1C peptide induces cell attachment and extracellular matrix deposition in lung fibroblasts. *Sci Rep* 5: 9496, 2015. doi:10.1038/srep09496.
10. **Ghavami S, Yeganeh B, Zeki AA, Shojaei S, Kenyon NJ, Ott S, Samali A, Patterson J, Alizadeh J, Moghadam AR, Dixon IMC, Unruh H, Knight DA, Post M, Klonisch T, Halayko AJ.** Autophagy and the unfolded protein response promote profibrotic effects of TGF-β1 in human lung fibroblasts. *Am J Physiol Lung Cell Mol Physiol* 314: L493–L504, 2018. doi:10.1152/ajplung.00372.2017.
11. **Haghi M, Traini D, Wood LG, Oliver B, Young PM, Chrzanowski W.** A 'soft spot' for drug transport: modulation of cell stiffness using fatty acids and its impact on drug transport in lung model. *J Mater Chem B Mater Biol Med* 3: 2583–2589, 2015. doi:10.1039/C4TB01928H.
12. **Hinz B, Celetta G, Tomasek JJ, Gabbiani G, Chaponnier C.** Alpha-smooth muscle actin expression upregulates fibroblast contractile activity. *Mol Biol Cell* 12: 2730–2741, 2001. doi:10.1091/mbc.12.9.2730.
13. **Hwang Y, Gouget CL, Barakat AI.** Mechanisms of cytoskeleton-mediated mechanical signal transmission in cells. *Commun Integr Biol* 5: 538–542, 2012. doi:10.4161/cib.21633.
14. **King TE Jr, Bradford WZ, Castro-Bernardini S, Fagan EA, Glaspole I, Glassberg MK, Gorina E, Hopkins PM, Kardatzke D, Lancaster L, Lederer DJ, Nathan SD, Pereira CA, Sahn SA, Sussman R, Swigris JJ, Noble PW; ASCEND Study Group.** A phase 3 trial of pirfenidone in patients with idiopathic pulmonary fibrosis. *N Engl J Med* 370: 2083–2092, 2014. doi:10.1056/NEJMoa1402582.
15. **Kirmizis D, Logothetidis S.** Atomic force microscopy probing in the measurement of cell mechanics. *Int J Nanomedicine* 5: 137–145, 2010. doi:10.2147/IJN.S5787.
16. **Kopycinska-Müller M, Geiss RH, Hurley DC.** Contact mechanics and tip shape in AFM-based nanomechanical measurements. *Ultramicroscopy* 106: 466–474, 2006. doi:10.1016/j.ultramic.2005.12.006.
17. **Kwok J, Grogan S, Meckes B, Arce F, Lal R, D'Lima D.** Atomic force microscopy reveals age-dependent changes in nanomechanical properties of the extracellular matrix of native human menisci: implications for joint degeneration and osteoarthritis. *Nanomedicine (Lond)* 10: 1777–1785, 2014. doi:10.1016/j.nano.2014.06.010.
18. **Ley B, Collard HR.** Epidemiology of idiopathic pulmonary fibrosis. *Clin Epidemiol* 5: 483–492, 2013. doi:10.2147/CLEP.S54815.
19. **Liu F, Lagares D, Choi KM, Stopfer L, Marinković A, Vrbanac V, Probst CK, Hiemer SE, Sisson TH, Horowitz JC, Rosas IO, Fredenburgh LE, Feghali-Bostwick C, Varelas X, Tager AM, Tschumperlin DJ.** Mechanosignaling through YAP and TAZ drives fibroblast activation and fibrosis. *Am J Physiol Lung Cell Mol Physiol* 308: L344–L357, 2015. doi:10.1152/ajplung.00300.2014.
20. **Liu F, Mih JD, Shea BS, Kho AT, Sharif AS, Tager AM, Tschumperlin DJ.** Feedback amplification of fibrosis through matrix stiffening and COX-2 suppression. *J Cell Biol* 190: 693–706, 2010. doi:10.1083/jcb.201004082.
21. **Liu F, Tschumperlin DJ.** Micro-mechanical characterization of lung tissue using atomic force microscopy. *J Vis Exp* 54: 2911, 2011. doi:10.3791/2911.
22. **Marinković A, Liu F, Tschumperlin DJ.** Matrices of physiologic stiffness potently inactivate idiopathic pulmonary fibrosis fibroblasts. *Am J Respir Cell Mol Biol* 48: 422–430, 2013. doi:10.1165/rcmb.2012-0335OC.
23. **Moreno-Herrero F, Colchero J, Gómez-Herrero J, Baró AM.** Atomic force microscopy contact, tapping, and jumping modes for imaging biological samples in liquids. *Phys Rev E Stat Nonlin Soft Matter Phys* 69: 031915, 2004. doi:10.1103/PhysRevE.69.031915.

24. **Parker MW, Rossi D, Peterson M, Smith K, Sikström K, White ES, Connett JE, Henke CA, Larsson O, Bitterman PB.** Fibrotic extracellular matrix activates a profibrotic positive feedback loop. *J Clin Invest* 124: 1622–1635, 2014. doi:10.1172/JCI71386.
25. **Raghu G, Collard HR, Egan JJ, Martinez FJ, Behr J, Brown KK, Colby TV, Cordier JF, Flaherty KR, Lasky JA, Lynch DA, Ryu JH, Swigris JJ, Wells AU, Ancochea J, Bouros D, Carvalho C, Costabel U, Ebina M, Hansell DM, Johkoh T, Kim DS, King TE Jr, Kondoh Y, Myers J, Müller NL, Nicholson AG, Richeldi L, Selman M, Dudden RF, Griss BS, Protzko SL, Schünemann HJ; ATS/ERS/JRS/ALAT Committee on Idiopathic Pulmonary Fibrosis.** An official ATS/ERS/JRS/ALAT statement: idiopathic pulmonary fibrosis: evidence-based guidelines for diagnosis and management. *Am J Respir Crit Care Med* 183: 788–824, 2011. doi:10.1164/rccm.2009-040GL.
26. **Richeldi L, du Bois RM, Raghu G, Azuma A, Brown KK, Costabel U, Cottin V, Flaherty KR, Hansell DM, Inoue Y, Kim DS, Kolb M, Nicholson AG, Noble PW, Selman M, Taniguchi H, Brun M, Le Maulf F, Girard M, Stowasser S, Schlenker-Herceg R, Disse B, Collard HR; INPULSIS Trial Investigators.** Efficacy and safety of nintedanib in idiopathic pulmonary fibrosis. *N Engl J Med* 370: 2071–2082, 2014. doi:10.1056/NEJMoa1402584.
27. **Roach KM, Wulff H, Feghali-Bostwick C, Amrani Y, Bradding P.** Increased constitutive αSMA and Smad2/3 expression in idiopathic pulmonary fibrosis myofibroblasts is KCa3.1-dependent. *Respir Res* 15: 155, 2014. doi:10.1186/s12931-014-0155-5.
28. **Ryerson CJ, Collard HR.** Update on the diagnosis and classification of ILD. *Curr Opin Pulm Med* 19: 453–459, 2013. doi:10.1097/MCP.0b013e328363f48d.
29. **Schulze C, Wetzel F, Kueper T, Malsen A, Muhr G, Jaspers S, Blatt T, Wittern K-P, Wenck H, Käs JA.** Stiffening of human skin fibroblasts with age. *Biophys J* 99: 2434–2442, 2010. doi:10.1016/j.bpj.2010.08.026.
30. **Thannickal VJ.** Mechanistic links between aging and lung fibrosis. *Biogerontology* 14: 609–615, 2013. doi:10.1007/s10522-013-9451-6.
31. **Thoelking G, Reiss B, Wegener J, Oberleithner H, Pavenstaedt H, Riethmuller C.** Nanotopography follows force in TGF-beta1 stimulated epithelium. *Nanotechnology* 21: 265102, 2010. doi:10.1088/0957-4484/21/26/265102.
32. **Weir JP.** Quantifying test-retest reliability using the intraclass correlation coefficient and the SEM. *J Strength Cond Res* 19: 231–240, 2005.
33. **Wells RG.** Tissue mechanics and fibrosis. *Biochim Biophys Acta* 1832: 884–890, 2013. doi:10.1016/j.bbadis.2013.02.007.